

Analytical method of computation of the thermal field in a DC lead with the variable heat transfer coefficient on its surface

Abstract. The thermal field of a DC lead with a variable coefficient of the heat transfer along its perimeter was investigated in the paper. Three different functions were assumed, which model the total heat transfer coefficient on the surface of a lead. In order to solve the problem of the two dimensional model an analytical method was developed (computer aided). It bases on superposition of the particular and general integral of the partial equation of heat conduction. The unknown coefficients of eigenfunctions and the constants of integration were determined in numerical way solving the adequate system of algebraic equations. Besides, the algorithm of computation of the steady-state current rating was presented. The obtained results were presented in a graphic form and verified by the method of finite elements.

Streszczenie. W pracy badano pole termiczne przewodu DC ze zmiennym współczynnikiem przejmowania ciepła na jego obwodzie. Założono przy tym trzy różne funkcje modelujące całkowity współczynnik przejmowania ciepła na powierzchni przewodu. W celu rozwiązywania dwuwymiarowego zagadnienia modelowego opracowano analityczną metodę (wspomaganą komputerowo). Bazuje ona na superpozycji całki szczególnej i ogólnej cząstkowego równania przewodnictwa cieplnego. Nieznane współczynniki funkcji własnych oraz stałe wyznaczono numerycznie rozwiązuając odpowiedni układ równań algebraicznych. Oprócz tego w pracy przedstawiono algorytm obliczania długotrwałej obciążalności prądowej. Otrzymane wyniki przedstawiono w postaci graficznej i zweryfikowano metodą elementów skończonych. (Analyticzna metoda obliczania pola temperatury w przewodzie DC ze zmiennym współczynnikiem przejmowania ciepła na jego powierzchni).

Keywords: DC lead, stationary thermal field, analytical methods, steady-state current rating.

Słowa kluczowe: przewód DC, stacjonarne pole termiczne, metody analityczne, długotrwały prąd dopuszczalny.

Introduction

Intensity of the convection around a horizontally placed cylinder depends on the location on its perimeter as it was shown by the results of many authors [1], [2]. The reason is because some kind of the thermal stream is formed right above the top of a lead [1] (Fig. 1). It results in worse heat exchange on the top and better one on the bottom. This phenomenon can be modeled by conditioning the coefficient of total heat transfer with respect to the angular coordinate. For such an approach axial symmetry of the field cannot be assumed. Boundary problem of the considered model becomes two dimensional for a sufficiently long conductor comparing with its diameter. It complicates analytical solution of the problem. On the other hand determination of the solution in the form of a formula is valuable and it brings much information. It enables discussion on the influence of particular parameters and physical interpretation of the obtained results, among others.

In the paper the thermal field of a DC lead with a variable coefficient of the heat transfer was investigated. An analytical method was developed, in which superposition of the particular and general integral of the partial equation of heat conduction was applied for the solution of the two dimensional boundary problem. The unknown coefficients of eigenfunctions and constants were determined from the solution of the adequate system of algebraic equations.

The important parameter of leads and cables is the steady-state current rating. For this reason additional algorithm was developed which determines the mentioned indicator.

Boundary problem of the model thermal field

The subject of investigations is a DC lead (Fig. 1) stranded of conducting bundles of a small diameter. The model of a homogeneous structure of the core was assumed for the analysis, but leading to the same thermal effects as in the real system. The mentioned condition is fulfilled for the identical current density in cross sections: $S_m = \pi R^2$ (see Fig. 1) and S_r (sum of the cross-sections of all bundles). Then the current I_m of the model should be reduced as follows

$$(1) \quad I_r = \frac{S_r}{S_m} I_m,$$

where I_r - real current in a lead.

It was assumed that the lead is placed in air of the temperature T_o . The system is shielded against the influence of direct sun radiation. The material parameters of a lead were averaged within the range $\langle T_o, T_{ll} \rangle$, where T_{ll} - maximum sustained temperature. The material parameters should be determined for T_{ll} in computations of the steady-state current rating.

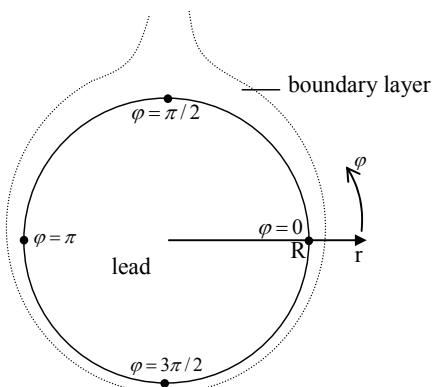


Fig. 1 Model of a lead with boundary layer [1]

Assuming the length of a lead much larger than its diameter and variable cooling conditions on its perimeter, the two dimensional equation of heat conduction was obtained [3], [4]

$$(2) \quad \frac{\partial^2 T(r, \varphi)}{\partial r^2} + \frac{1}{r} \frac{\partial T(r, \varphi)}{\partial r} + \frac{1}{r^2} \frac{\partial^2 T(r, \varphi)}{\partial \varphi^2} = -\frac{g}{\lambda}$$

for $0 \leq r \leq R$, $0 \leq \varphi \leq 2\pi$, where

$T(r, \varphi)$ - stationary temperature field, R - radius of a lead,

λ - specific thermal conductivity, $g = \frac{\rho I_m^2}{\pi^2 R^4}$ - efficiency of

spatial heat sources in the lead, ρ - specific resistivity of the lead, r - radial coordinate, φ - angular coordinate.

The external surface of a lead for $r = R$ gives up the heat by natural convection and radiation. The mentioned heat exchange is described by Hankel's boundary condition [5]

$$(3) \quad -\lambda \frac{\partial T(r, \varphi)}{\partial r} \Big|_{r=R} = \alpha(\varphi)[T(R, \varphi) - T_o].$$

In equation (3) the total heat transfer coefficient $\alpha(\varphi)$ depends on location on the perimeter of a lead.

Equations (2) and (3) determine the boundary problem of the investigated field.

Solution of the boundary problem

The particular integral of Poisson's equation (2) is known from the table placed in [12] (the case of the functions of variables r, φ of the cylindrical system). After reduction of the right side of (2) to zero, the general integral is determined by the separation of variables [6], [7]. After determination of eigenfunctions, the non-physical and singular solutions should be eliminated. The superposition of integrals leads to the following form of the solution

$$(4) \quad T(r, \varphi) = T_o + C - \frac{gr^2}{4\lambda} + \sum_{n=1}^{\infty} r^n [A_n \cos(n\varphi) + B_n \sin(n\varphi)]$$

for $0 \leq r \leq R$, $0 \leq \varphi \leq 2\pi$, where:

C - constant of integration, A_n, B_n - coefficients of eigenfunctions.

The next stage of the solution is determination of unknown coefficients A_n, B_n and constant C in relation (4).

In connection with that the summation of series (4) was reduced to the finite number L of terms and (4) was substituted to Hankel's boundary condition (3). In the result it was obtained:

$$(5) \quad -\frac{gR}{2\lambda} + \sum_{n=1}^L nR^{n-1} [A_n \cos(n\varphi) + B_n \sin(n\varphi)] = -\frac{\alpha(\varphi)}{\lambda} \left\{ C - \frac{gR^2}{4\lambda} + \sum_{n=1}^L R^n [A_n \cos(n\varphi) + B_n \sin(n\varphi)] \right\}.$$

Then relation (5) was multiplicated by $\cos(m\varphi)$ and integrated by sides with respect to the angular coordinate φ in the range $\langle 0, 2\pi \rangle$. This way equation (6a) was obtained for $m = 1, 2, \dots, L$. Next equation was obtained multiplicating (5) by $\sin(m\varphi)$ and integrating by sides with respect to the same coordinate and the same range as in the above. In the result one comes to equation (6b) for $m = 1, 2, \dots, L$. The last equation (6c) was obtained in the result of integration the both sides of relation (5) with respect to the angular coordinate φ in the range $\langle 0, 2\pi \rangle$. In computing integrals appearing in (6a,b) orthogonality condition of the system of functions $\{\cos(m\varphi), \sin(m\varphi)\}$ in the range $\langle 0, 2\pi \rangle$ was applied. In the result relations (6a-c) form the system of $2L+1$ equations with respect to A_n, B_n, C .

$$\begin{cases} \sum_{n=1}^L A_n I_1(m, n) + \sum_{n=1}^L B_n I_2(m, n) + C I_3(m) = \frac{gR^2}{4\lambda} I_3(m), & m = 1, 2, \dots, L, \\ \sum_{n=1}^L A_n I_4(m, n) + \sum_{n=1}^L B_n I_5(m, n) + C I_6(m) = \frac{gR^2}{4\lambda} I_6(m), & m = 1, 2, \dots, L, \\ \sum_{n=1}^L A_n I_7(n) + \sum_{n=1}^L B_n I_8(n) + C I_9 = \frac{gR\pi}{\lambda} + \frac{gR^2}{4\lambda} I_9 \end{cases}$$

(6a,b,c) where:

$$I_1(m, n) = \begin{cases} \frac{R^n}{\lambda} \int_0^{2\pi} \alpha(\varphi) \cos(n\varphi) \cos(m\varphi) d\varphi & \text{for } m \neq n \\ \frac{R^m}{\lambda} \int_0^{2\pi} \alpha(\varphi) \cos^2(m\varphi) d\varphi + m\pi R^{m-1} & \text{for } m = n, \end{cases}$$

(7a)

$$I_2(m, n) = \frac{R^n}{\lambda} \int_0^{2\pi} \alpha(\varphi) \sin(n\varphi) \cos(m\varphi) d\varphi,$$

(7b)

$$I_3(m) = \frac{1}{\lambda} \int_0^{2\pi} \alpha(\varphi) \cos(m\varphi) d\varphi,$$

(7c)

$$I_4(m, n) = \frac{R^n}{\lambda} \int_0^{2\pi} \alpha(\varphi) \cos(n\varphi) \sin(m\varphi) d\varphi,$$

(8a)

$$I_5(m, n) = \begin{cases} \frac{R^n}{\lambda} \int_0^{2\pi} \alpha(\varphi) \sin(n\varphi) \sin(m\varphi) d\varphi & \text{for } m \neq n \\ \frac{R^m}{\lambda} \int_0^{2\pi} \alpha(\varphi) \sin^2(m\varphi) d\varphi + m\pi R^{m-1} & \text{for } m = n, \end{cases}$$

(8b)

$$I_6(m) = \frac{1}{\lambda} \int_0^{2\pi} \alpha(\varphi) \sin(m\varphi) d\varphi,$$

(8c)

$$I_7(n) = \frac{R^n}{\lambda} \int_0^{2\pi} \alpha(\varphi) \cos(n\varphi) d\varphi,$$

(9a)

$$I_8(n) = \frac{R^n}{\lambda} \int_0^{2\pi} \alpha(\varphi) \sin(n\varphi) d\varphi,$$

(9b)

$$I_9 = \frac{1}{\lambda} \int_0^{2\pi} \alpha(\varphi) d\varphi.$$

(9c)

The computation of integrals (7-9) for the given $\alpha(\varphi)$ leads to determination of unknown coefficients A_n, B_n and the constant C from the system of equations (6). The results of computations of the integrals (7-9) for three different functions $\alpha(\varphi)$ were placed in the appendix.

Steady-state current rating

One of the most important parameters of leads and cables is the steady-state current rating I_{rl} . It is bounded by the highest value of the temperature T_{ll} , to which the lead can be heated up in the terms of sustained operation. In order to determine I_{rl} such a highest value of the current I_{ml} should be found, for which the highest temperature of the lead surface (i.e. for $r = R$) will not exceed T_{ll} . Because of the assumed approximations of the heat transfer coefficient $\alpha(\varphi)$ (where the worst give up of the heat takes place on the top of a lead), the angular coordinate of the warmest point is $\varphi = \pi/2$. Because the temperature is a rising function of the current intensity, it is sufficient to solve the following equation with respect to I_{ml}

$$(10) \quad T(r = R, \varphi = \pi/2, I_{ml}) = T_{ll}.$$

For this purpose the algorithm was developed, which block diagram is shown in Fig. 2. It consists of:

I) block of investigations of the starting interval $\langle I_a, I_b \rangle$,

II) block of investigations of the sustained current intensity I_{rl} .

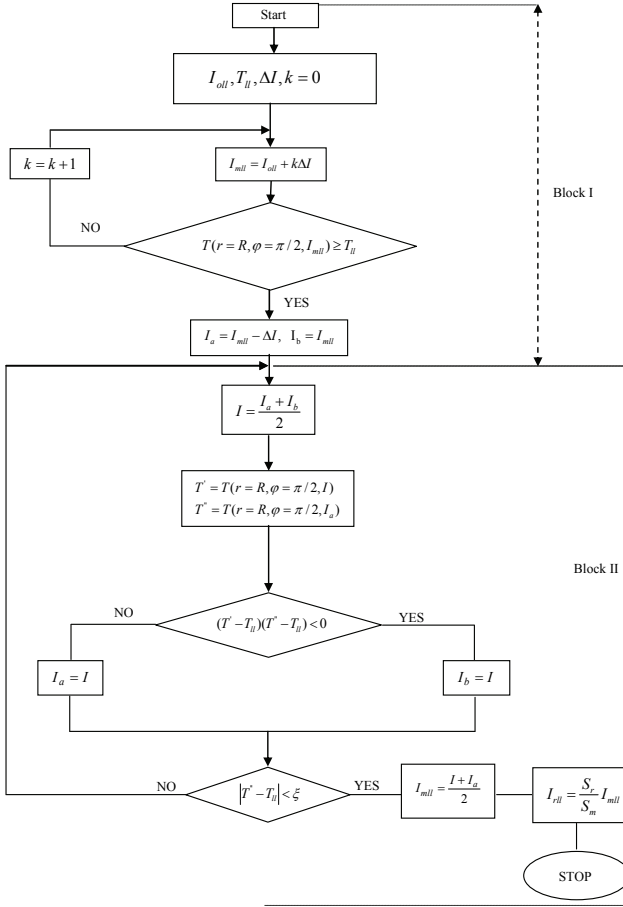


Fig. 2 Block diagram of the simplified algorithm for determination of the steady-state current rating

In block I the current intensity I_{mll} is increased with the constant step ΔI (Fig. 2). After satisfying condition

$T(R, \frac{\pi}{2}, I_{mll}) \geq T_{ll}$ the right boundary of the interval I_b is founded. The left boundary I_a is determined by subtraction of the step ΔI .

In block II the current I_{mll} is investigated in the range $\langle I_a, I_b \rangle$ by the method of bisection [8], [13]. In the mentioned block, after sectioning of the range the auxiliary temperatures T', T'' are determined, among others (for different currents). They are used to control decrease of the width of the range (see Fig. 2). In the result, after satisfying condition $|T'' - T_{ll}| < \xi$ in the consecutive iteration, the admissible sustained current is determined.

Computational examples

The computer programme was prepared taking advantage of the package Mathematica [9]. It computes the temperature distribution of a lead and the steady-state current rating. The copper lead was analyzed of the real cross section $S_r = 300 \text{ mm}^2$. The following data were assumed:

$$R = 0,01125 \text{ m}, \lambda = 360 \text{ W/(mK)}, T_o = 25^\circ\text{C}, T_{ll} = 80^\circ\text{C}, \rho = 2,16 \cdot 10^{-8} \Omega \text{m}, \Delta I = 10 \text{ A}, \xi = 0,01^\circ\text{C}, L = 15. \quad (11)$$

Three different functions $\alpha(\varphi)$ were assumed subsequently. They model the total heat transfer coefficient on the lead surface. The first approximation $\alpha_1(\varphi)$ was determined on the basis of the relations from monography [2]. They are relatively accurate and they consider the diameter of a lead and relative criterial numbers (Nusselt's, Rayeleigh's, Prandtl's) [1], [2], as well. It leads to the following relations

$$\alpha_1(\varphi) = (\alpha_{\max} - \alpha_{\min})(1 - e^{\frac{\varphi - \pi/2}{B}}) + \alpha_{\min} \text{ for } \varphi \in \langle 0, \pi/2 \rangle$$

$$\alpha_1(\varphi) = (\alpha_{\max} - \alpha_{\min})(1 - e^{\frac{-\varphi + \pi/2}{B}}) + \alpha_{\min} \text{ for } \varphi \in \langle \pi/2, 3\pi/2 \rangle$$

$$\alpha_1(\varphi) = (\alpha_{\max} - \alpha_{\min})(1 - e^{\frac{\varphi - 5\pi/2}{B}}) + \alpha_{\min} \text{ for } \varphi \in \langle 3\pi/2, 2\pi \rangle,$$

where: $\alpha_{\max} = 18,2 \text{ W}/(\text{m}^2 \text{K})$, $\alpha_{\min} = 9,8 \text{ W}/(\text{m}^2 \text{K})$, $B = 0,85$. (12)

Fig. 3 was prepared based on (12), which illustrates, among others, the distribution of coefficient $\alpha_1(\varphi)$ in the function of angular coordinate. In the second approximation $\alpha_2(\varphi)$ the constant value of the coefficient was assumed on the upper half of a lead and the constant value (but larger) on the bottom half

$$(13) \quad \alpha_2(\varphi) = \begin{cases} 13 \text{ W}/(\text{m}^2 \text{K}) & \text{for } 0 < \varphi < \pi \\ 19 \text{ W}/(\text{m}^2 \text{K}) & \text{for } \pi < \varphi < 2\pi. \end{cases}$$

The above equation models better give up of the heat by the lower surface of a lead than by the upper one. In the third case the same heat exchange was considered assuming $\alpha_3(\varphi) = \text{const} = 16 \text{ W}/(\text{m}^2 \text{K})$ along the whole perimeter of a lead. Averaging functions $\alpha_1(\varphi), \alpha_2(\varphi), \alpha_3(\varphi)$ on the perimeter of a lead gives the same $\alpha_{sr} = 16 \text{ W}/(\text{m}^2 \text{K})$ in the three considered cases. The diagrams of functions $\alpha_2(\varphi), \alpha_3(\varphi)$ were shown in Fig. 3, as well.

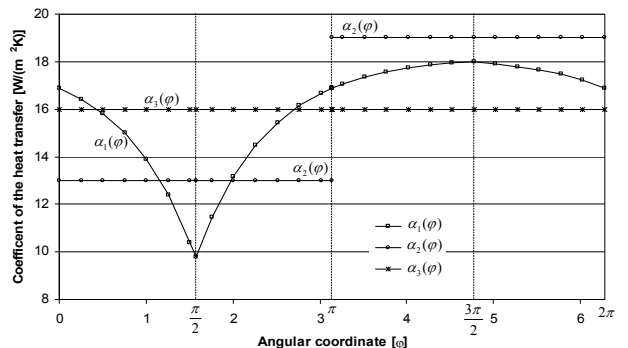


Fig. 3 Coefficients of the heat transfer $\alpha_1(\varphi), \alpha_2(\varphi), \alpha_3(\varphi) = \text{const}$ in the function of angular coordinate

The results of computations of the field distributions for $\alpha_1(\varphi), \alpha_2(\varphi), \alpha_3(\varphi) = \text{const}$ were presented in the respective diagrams. Temperature distributions along the perimeter of a lead ($r = R$) were shown (see fig. 4) in the function of the angular coordinate for the load of the system by the steady-state current rating. Fig. 5 illustrates temperature distributions in the function of relative radial coordinate for the constant value of the angular coordinate $\varphi = \pi/2$ with the load of the steady-state current rating, as

well. In Tab. 1 admissible sustained currents were shown for all considered coefficients of the heat transfer.

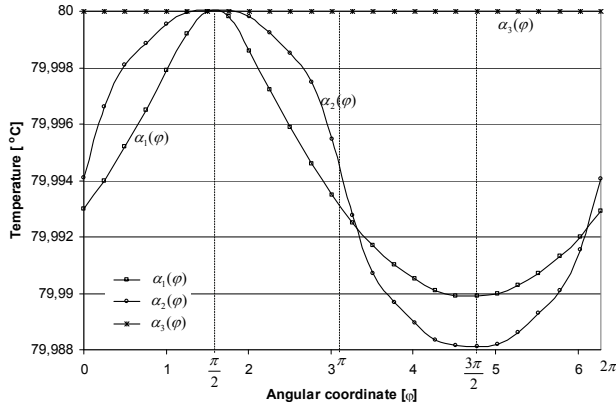


Fig. 4 Temperature distributions along the perimeter of a lead ($r = R$) in the function of the angular coordinate with the load given in Tab. 1

Tab.1 Steady-state current ratings for three considered coefficients of the heat transfer

Model of the heat coefficient transfer	Steady-state current rating I_{rl} [A]
$\alpha_1(\varphi)$	806,91
$\alpha_2(\varphi)$	807,32
$\alpha_3(\varphi) = \text{const}$	807,37

The presented analytical method had to be verified. For this reason the obtained results were compared with computations made by the finite element method FE [10]. It is the base of the programme NISA/HEAT Transfer [11], which was utilized for verification. The two dimensional model of a lead was approximated by the mesh consisting of 900 elements and 2983 nodes. In Fig. 6 the relative differences of distributions

$$(14) \quad 100\% \frac{T_{FE}(r, \varphi) - T_{AN}(r, \varphi)}{T_{FE}(r, \varphi)}$$

were illustrated, where

$T_{FE}(r, \varphi)$ - temperature distribution obtained by the method of finite elements, $T_{AN}(r, \varphi)$ - temperature distribution obtained by the developed analytical method.

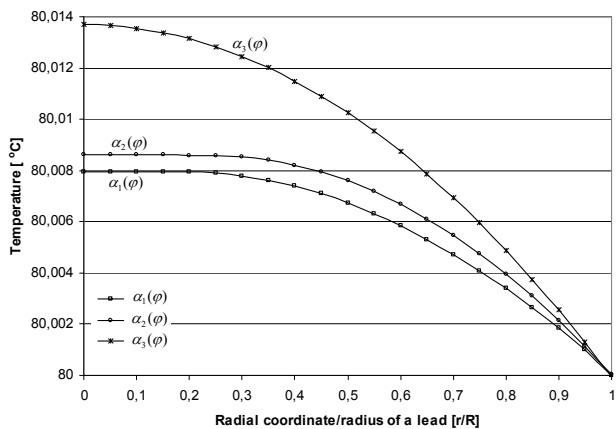


Fig. 5 Temperature distributions in the lead in the function of the relative radial coordinate r/R for $\varphi = \pi/2$ with the load given in Tab. 1

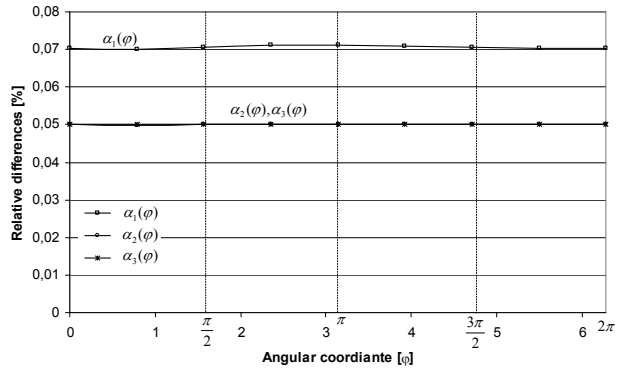


Fig. 6 Relative differences of the temperature distributions obtained by the method of finite elements and the analytical one along the perimeter of a lead ($r = R$) in the function of angular coordinate

Conclusions

A) From Tab. 1 follows, that the steady-state current ratings for all considered coefficients of the heat transfer $\alpha_1(\varphi), \alpha_2(\varphi), \alpha_3(\varphi) = \text{const}$ are very close to each other. It is caused because of the same averaged value of functions $\alpha_1(\varphi), \alpha_2(\varphi)$ and $\alpha_3(\varphi)$ along the perimeter of a lead. It follows from the above, that averaged value of the heat transfer coefficient along the perimeter of a lead can be assumed for computations. Such an approach significantly simplifies the analysis causing that two dimensional boundary problem is reduced to the one dimensional.

B) Some differences are observed for $\alpha_1(\varphi)$ between temperature values at the highest ($\varphi = \pi/2$) and the lowest placed points ($\varphi = 3\pi/2$) (Fig. 4 for $\alpha_1(\varphi)$, analysing distributions in the function of angular coordinate $T(r = R, \varphi)$). A similar effect takes place for $\alpha_2(\varphi)$, as well (Fig. 4). It is caused by assumed approximations of the heat transfer coefficient, which models influence of the boundary layer, more or less. For a constant value of the heat transfer coefficient $\alpha_3(\varphi)$, the temperature of the lead surface is uniform (Fig. 4 for $\alpha_3(\varphi) = \text{const.}$). On the other hand with increase of the radial coordinate (and a constant value of the angular coordinate) the temperature value of a lead decreases for all assumed coefficients of the heat transfer (Fig. 5). The temperature decrease along the whole radius is rather small (e.g. $T(r=0, \varphi=\pi/2) - T(r=R, \varphi=\pi/2) \leq 0.08^\circ\text{C}$ with $\alpha_1(\varphi)$). Very small changes of the temperature in a lead are caused mainly by the large thermal conductivity of copper.

C) Relative differences (14) of the temperature distributions computed by the finite element method (FE) and the analytical one (AN) are the largest for the heat transfer coefficient $\alpha_1(\varphi)$ (Fig. 6 for $r = R$). The maximum is equal to 0.072% for $\varphi \approx 3\pi/4$. Differences are less for the remained coefficients of the heat transfer. Discussed deviations at other points of the lead ($r < R$) are almost the same as those presented in Fig. 6. Then the developed method should be considered as verified.

ACKNOWLEDGEMENT

The paper was prepared at Białystok Technical University within a framework of the S/WE/3/08 project sponsored by the Ministry of Science and Higher Education, Poland.

REFERENCES

- [1] Incropera F. P., de Witt D. P., Bergman T. L., Lavine A. S., *Introduction to heat transfer*, Wiley, New York, NY 2007.
- [2] Gołębowski J., Kwieckowski S., Zaręba M., Bycul R. P., *Analiza niewielkiego pola termicznego w elektrycznych grzejnikach podlogowych i w kablach prądu stałego*, (Analysis of the transient thermal field in electrical floor heaters and in DC cables), Oficyna Wydawnicza Politechniki Białostockiej, Warszawa-Białystok 2010, Polska Akademia Nauk – Komitet Elektrotechniki (in Polish).
- [3] Beck J. V., Cole K. D., Haji-Sheikh A., Litkouhi B., *Heat conduction using Green's functions*, Hemisphere Publishing Corporation, London-Philadelphia 1992.
- [4] Baehr M. D., Stephan K., *Heat and mass transfer*, Springer-Verlag, Berlin, Heidelberg 2006.
- [5] Taler J., Duda P., *Rozwiązywanie prostych i odwrotnych zagadnień przewodzenia ciepła*, (Solving direct and inverse problems of heat conduction), WNT, Warszawa 2003 .
- [6] Lehner G., *Electromagnetische Feldtheorie für Ingenieure und Physiker*, Springer Verlag, Berlin, Heidelberg 1996.
- [7] Evans L. C., *Równania różniczkowe cząstkowe*, (Partial differential equations), WNT, Warszawa 2002 (in Polish).
- [8] Fortuna Z., Macukow B., Wąsowski J., *Metody numeryczne*, (Numerical methods), WNT, Warszawa 1993 (in Polish).
- [9] Grzymkowski R., Kapusta A., Kumoszek T., Siota D., *Mathematica 6*, Wydawnictwa Pracowni Komputerowej Jacka Skalmierskiego, Gliwice 2008 (in Polish).
- [10] Bathe K. J., *Finite-Elemente Methoden*, Springer-Verlag, Berlin 1990.
- [11] Manuals for NISA v. 16, NISA Suite of FEA Software (CD-ROM), Cranes Software, Inc., Troy, MI 2008.
- [12] Matusiak R., *Elektrotechnika teoretyczna. Tom 2. Teoria pola elektromagnetycznego*, (Theoretical elecrotechnics. Vol 2. Electromagnetic field theory), WNT, Warszawa 1982 .
- [13] Gołębowski J., Bycul R. P., Thermal analysis of short-circuit and cooling states in a DC cable with the use of parallel computations, *Przegląd Elektrotechniczny – Electrical Review*, 85 (2009), No. 10, 95-100.

Appendix

Results of the computation of integrals (7-9) for the heat transfer coefficient $\alpha_1(\varphi)$:

$$I_1(m, n) = BR^n \frac{(\alpha_{\max} - \alpha_{\min})}{\lambda} \left[\frac{e^{-\frac{\pi}{B}} \cos \frac{3\pi(m-n)}{2} - \cos \frac{(m-n)\pi}{2}}{B^2(m-n)^2 + 1} + \right. \\ \left. + \frac{e^{-\frac{\pi}{B}} \cos \frac{3\pi(m+n)}{2} - \cos \frac{(m+n)\pi}{2}}{B^2(m+n)^2 + 1} \right] \quad \text{for } m \neq n,$$
 (A1)

$$I_1(m, n) = \frac{e^{-\frac{\pi}{B}} R^m}{\lambda(4B^2 m^2 + 1)} \left[B(\alpha_{\max} - \alpha_{\min})(1 + 4B^2 m^2 + (-1)^m) + \right. \\ \left. + e^{\frac{\pi}{B}} ((4B^2 m^2 + 1)(\pi\alpha_{\max} - B(\alpha_{\max} - \alpha_{\min})) - B(-1)^m(\alpha_{\max} - \alpha_{\min})) \right] + m\pi R^{m-1} \quad \text{for } m = n,$$
 (A2)

$$I_2(m, n) = \frac{BR^n e^{-\frac{\pi}{B}} (\alpha_{\max} - \alpha_{\min})}{\lambda} \left[\frac{\sin \frac{\pi(m-n)}{2} (e^{\frac{\pi}{B}} - 1 - 2 \cos((m-n)\pi))}{B^2(m-n)^2 + 1} + \right. \\ \left. + \frac{\sin \frac{3\pi(m+n)}{2} - e^{\frac{\pi}{B}} \sin \frac{(m+n)\pi}{2}}{B^2(m+n)^2 + 1} \right], \quad \text{for } m \neq n,$$
 (A3)

$$I_3(m) = \frac{2Be^{-\frac{\pi}{B}} (\alpha_{\max} - \alpha_{\min})}{\lambda} \left[\frac{2(-1)^m - 1 - e^{\frac{\pi}{B}}}{B^2 m^2 + 1} \right] \cos\left(\frac{m\pi}{2}\right), \quad \text{for } m = n,$$
 (A4)

$$I_4(m, n) = BR^n \frac{(\alpha_{\max} - \alpha_{\min})}{\lambda} \left[\frac{e^{-\frac{\pi}{B}} \sin \frac{3\pi(m-n)}{2} - \sin \frac{(m-n)\pi}{2}}{B^2(m-n)^2 + 1} + \right. \\ \left. + \frac{e^{-\frac{\pi}{B}} \sin \frac{3\pi(m+n)}{2} - \sin \frac{(m+n)\pi}{2}}{B^2(m+n)^2 + 1} \right], \quad \text{for } m \neq n,$$
 (A5)

$$I_5(m, n) = \frac{BR^n (\alpha_{\max} - \alpha_{\min})}{\lambda} \left[\frac{e^{-\frac{\pi}{B}} \cos \frac{3\pi(m-n)}{2} - \cos \frac{(m-n)\pi}{2}}{B^2(m-n)^2 + 1} + \right. \\ \left. + \frac{\cos \frac{\pi(m+n)}{2} - e^{-\frac{\pi}{B}} \cos \frac{3(m+n)\pi}{2}}{B^2(m+n)^2 + 1} \right]$$
 (A6)

for $m \neq n$,

$$I_5(m, n) = \frac{e^{-\frac{\pi}{B}} R^m}{\lambda(4B^2 m^2 + 1)} \left[B(\alpha_{\max} - \alpha_{\min})(1 + 4B^2 m^2 + (-1)^m) + \right. \\ \left. + e^{\frac{\pi}{B}} (B(-1)^m(\alpha_{\max} - \alpha_{\min}) + (4B^2 m^2 + 1)(\pi\alpha_{\max} - B(\alpha_{\max} - \alpha_{\min}))) \right] + m\pi R^{m-1}$$
 (A7)

$$I_6(m) = \frac{2Be^{-\frac{\pi}{B}} (\alpha_{\max} - \alpha_{\min})}{\lambda} \left[\frac{1 + 2(-1)^m - e^{\frac{\pi}{B}}}{B^2 m^2 + 1} \right] \sin\left(\frac{m\pi}{2}\right), \quad \text{for } m = n,$$
 (A8)

$$I_7(n) = \frac{2BR^n e^{-\frac{\pi}{B}} (\alpha_{\max} - \alpha_{\min})}{\lambda} \left[\frac{2(-1)^n - 1 - e^{\frac{\pi}{B}}}{B^2 n^2 + 1} \right] \cos\left(\frac{n\pi}{2}\right), \quad \text{for } m = n,$$
 (A9)

$$I_8(n) = \frac{2BR^n e^{-\frac{\pi}{B}} (\alpha_{\max} - \alpha_{\min})}{\lambda} \left[\frac{1 + 2(-1)^n - e^{\frac{\pi}{B}}}{B^2 n^2 + 1} \right] \sin\left(\frac{n\pi}{2}\right), \quad \text{for } m = n,$$
 (A10)

$$I_9 = \frac{2B}{\lambda} (\alpha_{\max} - \alpha_{\min}) (e^{-\frac{\pi}{B}} - 1) + \frac{2\pi}{\lambda} \alpha_{\max}. \quad \text{for } m = n,$$
 (A11)

Results of the computation of integrals (7-9) for the heat transfer coefficient $\alpha_2(\varphi)$:

$$(A12) I_1(m, n) = \begin{cases} 0 & \text{for } m \neq n \\ \frac{\pi R^m (\alpha_{\max} + \alpha_{\min})}{2\lambda} + m\pi R^{m-1} & \text{for } m = n, \end{cases}$$

$$(A13) I_2(m, n) = \begin{cases} \frac{nR^n (\alpha_{\max} - \alpha_{\min})}{\lambda(n^2 - m^2)} ((-1)^{m+n} - 1) & \text{for } m \neq n \\ 0 & \text{for } m = n, \end{cases}$$
 (A14)

$$I_3(m) = 0,$$

$$(A15) I_4(m,n) = \begin{cases} \frac{mR^n(\alpha_{\max} - \alpha_{\min})}{\lambda(m^2 - n^2)} ((-1)^{m+n} - 1) & \text{for } m \neq n \\ 0 & \text{for } m = n, \end{cases}$$

$$(A16) \quad I_5(m,n) = I_1(m,n),$$

$$(A17) \quad I_6(m) = \frac{2[\alpha_{\max} + \alpha_{\min} + 2(-1)^m \alpha_{\max}] \sin^2(\frac{m\pi}{2})}{m\lambda},$$

$$(A18), \quad I_7(n) = 0,$$

$$(A19) \quad I_8(n) = \frac{2R^n[\alpha_{\max} + \alpha_{\min} + 2(-1)^n \alpha_{\max}] \sin^2(\frac{n\pi}{2})}{n\lambda},$$

$$(A20) \quad I_9 = \frac{\pi(\alpha_{\max} + \alpha_{\min})}{\lambda}.$$

$$(A21) \quad I_1(m,n) = \begin{cases} 0 & \text{for } m \neq n \\ \frac{\pi R^m \alpha}{\lambda} + m\pi R^{m-1} & \text{for } m = n, \end{cases}$$

$$(A22) \quad I_2(m,n) = 0,$$

$$(A23) \quad I_3(m) = 0,$$

$$(A24) \quad I_4(m,n) = 0,$$

$$(A25) \quad I_5(m,n) = I_1(m,n),$$

$$(A26) \quad I_6(m) = 0,$$

$$(A27) \quad I_7(n) = I_8(n) = 0,$$

$$(A28) \quad I_9 = \frac{2\pi\alpha}{\lambda}.$$

Results of the computation of integrals (7-9) for the heat transfer coefficient $\alpha_3(\varphi) = \alpha = \text{const}$:

Authors: Prof. J. Golebiowski¹, M. Zaręba², Ph. D., Białystok Technical University, Faculty of Electrical Engineering, Wiejska 45D st., 15-351 Białystok, e-mail: ¹ goleb@we.pb.edu.pl, ² m.zareba@we.pb.edu.pl